High-Throughput Nano-Biofilm Microarray for Antifungal Drug Discovery

Anand Srinivasan,[a,c] Kai P. Leung,[d] Jose L. Lopez-Ribot,[b,c] Anand K. Ramasubramanian[a,c]

Departments of Biomedical Engineering[a] and Biology[b] and South Texas Center for Emerging Infectious Diseases,[c] The University of Texas at San Antonio, San Antonio, Texas, USA; U.S. Army Dental and Trauma Research Detachment, Institute of Surgical Research, Fort Sam Houston, San Antonio, Texas, USA[d]

ABSTRACT **Micro- and nanoscale technologies have radically transformed biological research from genomics to tissue engineering, with the relative exception of microbial cell culture, which is still largely performed in microtiter plates and petri dishes. Here, we present nanoscale culture of the opportunistic fungal pathogen *Candida albicans* on a microarray platform. The microarray consists of 1,200 individual cultures of 30 nl of *C. albicans* biofilms ("nano-biofilms") encapsulated in an inert alginate matrix. We demonstrate that these nano-biofilms are similar to conventional macroscopic biofilms in their morphological, architectural, growth, and phenotypic characteristics. We also demonstrate that the nano-biofilm microarray is a robust and efficient tool for accelerating the drug discovery process: (i) combinatorial screening against a collection of 28 antifungal compounds in the presence of immunosuppressant FK506 (tacrolimus) identified six drugs that showed synergistic antifungal activity, and (ii) screening against the NCI challenge set small-molecule library identified three heretofore-unknown hits. This cell-based microarray platform allows for miniaturization of microbial cell culture and is fully compatible with other high-throughput screening technologies.**

IMPORTANCE **Microorganisms are typically still grown in petri dishes, test tubes, and Erlenmeyer flasks in spite of the latest advances in miniaturization that have benefitted other allied research fields, including genomics and proteomics. Culturing microorganisms in small scale can be particularly valuable in cutting down time, cost, and reagent usage. This paper describes the development, characterization, and application of nanoscale culture of an opportunistic fungal pathogen, *Candida albicans*. Despite a more than 2,000-fold reduction in volume, the growth characteristics and drug response profiles obtained from the nanoscale cultures were comparable to the industry standards. The platform also enabled rapid identification of new drug candidates that were effective against *C. albicans* biofilms, which are a major cause of mortality in hospital-acquired infections.**

Received 30 April 2013 **Accepted** 23 May 2013 **Published** 25 June 2013

Citation Srinivasan A, Leung KP, Lopez-Ribot JL, Ramasubramanian AK. 2013. High-throughput nano-biofilm microarray for antifungal drug discovery. mBio 4(4):e00331-13. doi:10.1128/mBio.00331-13.

Editor Joseph Heitman, Duke University

Address correspondence to Anand K. Ramasubramanian, anand.ramasubramanian@utsa.edu, or Jose L.Lopez-Ribot, jose.lopezribot@utsa.edu.

Infectious diseases are still a major cause of morbidity and mortality today (1–4). Antibiotic therapy remains the mainstay for the treatment of these infections. Nevertheless, its success is severely hampered by frequent development of new strains or organisms with increased drug resistance, as well as tissue and organ toxicity at higher doses. In addition, there is a lack of new antibiotics in the pipeline of most major pharmaceutical companies (5). A major impediment to the development of newer antibiotics is the fact that classical microbiological culture techniques are mostly incompatible with the high-throughput screening (HTS) technologies that have recently dominated drug discovery, genomics, and proteomics. While microorganisms are still typically cultured in flasks, tubes, and plates with volumes ranging from liters down to milliliters, the modern HTS techniques span the range from milliliters down to picoliters. Thus, the throughput of conventional microbial culture techniques is lagging behind by at least 3 to 6 orders of magnitude.

Over the past decade, forays into exploring applications of nanotechnology in microbial cell culture have been reassuring, particularly with respect to increasing our understanding of the microbial world (6–8). Culturing microorganisms in nanoscale has enabled us to investigate how individual organisms or organisms in a select population interact with their environment, such as quorum sensing (9, 10), response to spatial confinement (11), motility and chemotaxis (12), antibiotic susceptibility (13–16), and cellular physiology (17). However, the vast potential of micro- and nanoscale cultures remains underdeveloped for clinical and translational purposes such as drug discovery and diagnostics.

In this work, we have addressed the knowledge and technological gaps by developing a robust, universal platform for high-throughput microbial culture and demonstrating its utility for drug discovery. We employed the opportunistic fungal pathogen *Candida albicans*, which is the most common cause of nosocomial (i.e., hospital-acquired) fungal infection, with an unacceptably high mortality rate of 40% to 60% in disseminated invasive candidiasis (4). In many situations, *C. albicans* is associated with the formation of biofilm commonly found on implanted biomaterials and host surfaces. One of the reasons for such a high rate of mortality in the case of invasive candidiasis is the lack of effective

Report Documentation Page

Form Approved
OMB No. 0704-0188

1. REPORT DATE	2. REPORT TYPE	3. DATES COVERED
01 JUL 2013	**N/A**	**-**

4. TITLE AND SUBTITLE	5a. CONTRACT NUMBER
High-Throughput Nano-Biofilm Microarray for Antifungal Drug Discovery	5b. GRANT NUMBER
	5c. PROGRAM ELEMENT NUMBER
6. AUTHOR(S)	5d. PROJECT NUMBER
Srinivasan A., Leung K. P., Lopez-Ribot J. L., Ramasubramanian A. K.,	5e. TASK NUMBER
	5f. WORK UNIT NUMBER
7. PERFORMING ORGANIZATION NAME(S) AND ADDRESS(ES)	8. PERFORMING ORGANIZATION REPORT NUMBER
United States Army Institute ofSurgical Research, JBSA Fort Sam Houston, TX	
9. SPONSORING/MONITORING AGENCY NAME(S) AND ADDRESS(ES)	10. SPONSOR/MONITOR'S ACRONYM(S)
	11. SPONSOR/MONITOR'S REPORT NUMBER(S)

12. DISTRIBUTION/AVAILABILITY STATEMENT
Approved for public release, distribution unlimited

13. SUPPLEMENTARY NOTES

14. ABSTRACT

15. SUBJECT TERMS

16. SECURITY CLASSIFICATION OF:			17. LIMITATION OF ABSTRACT	18. NUMBER OF PAGES	19a. NAME OF RESPONSIBLE PERSON
a. REPORT	b. ABSTRACT	c. THIS PAGE			
unclassified	**unclassified**	**unclassified**	**UU**	**11**	

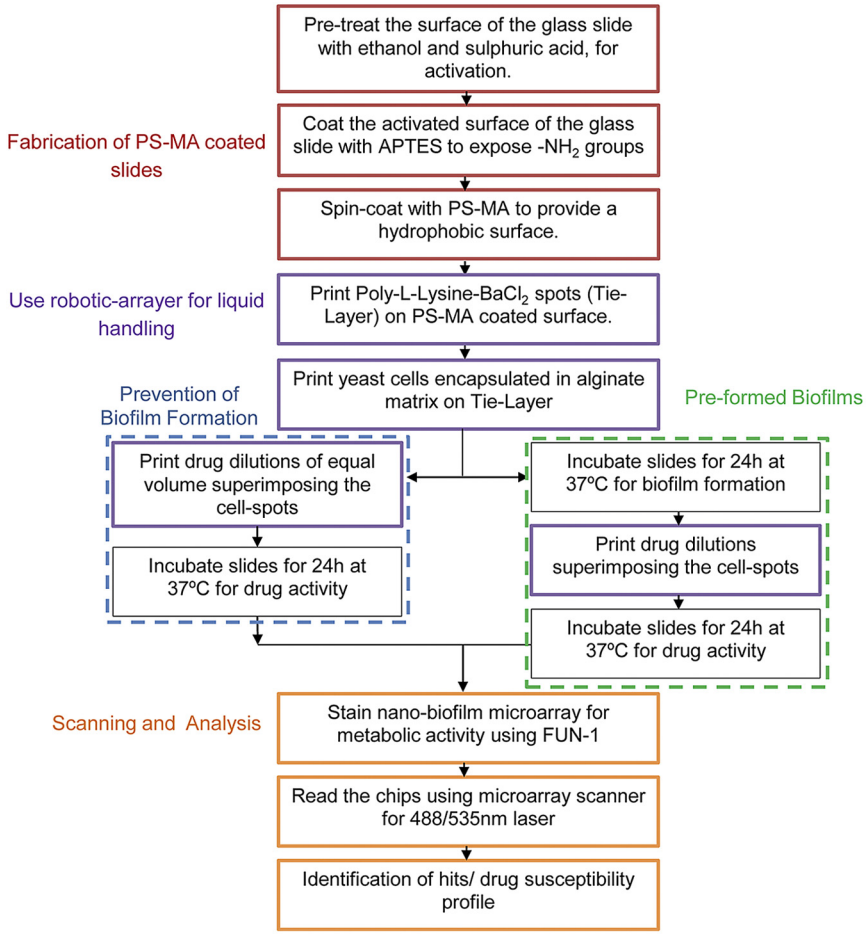

FIG 1 Schematic of workflow in the fabrication of nano-biofilm microarray and associated drug screening process to identify antifungal drugs that inhibit biofilm formation and act against preformed biofilms.

antifungal drugs against the highly protective structured population of *C. albicans*. We have fabricated a cellular microarray system consisting of nanoscale cultures of *C. albicans* biofilms ("nano-biofilms") encapsulated in a chemically inert alginate matrix. This platform is based on our recent report on the encapsulation of *C. albicans* biofilms in collagen gels, which had limited applicability due to its gelation and drug binding properties (18). Here, we demonstrate that despite more than 3 orders of magnitude of miniaturization, the nano-biofilms maintain their growth and phenotypic characteristics comparably to industry-standard large-scale cultures. We also demonstrate that nano-biofilm microarrays can be used for efficient and rapid screening of small-molecule libraries of novel antifungal drug candidates, either singly or combinatorially. We anticipate that this microarray platform will transform the paradigm and practice of microbial cell culture, drug screening, and diagnostics.

RESULTS AND DISCUSSION

The process of developing a nano-biofilm microarray for *C. albicans* to screen for drug candidates or combinations of drugs with novel antifungal properties consisted of the following sequential steps: (i) modification of glass surface; (ii) optimization of culture conditions for biofilm formation; (iii) exposure of biofilms to drug candidates; and (iv) analysis of cell viability and drug susceptibility (Fig. 1).

Modification of glass surface. We fabricated the microarray on modified glass substrates following a procedure previously developed by us (18). Microscope glass slides were modified by a series of chemical processing steps, and at each step, the surface was analyzed by Fourier transform infrared (FTIR) spectroscopy to determine the molecular structure on the surface. The molecular structure can be recognized from the absorption bands in the mid-infrared region (4,000 to 400 cm^{-1}) characteristic of the vibrational frequencies of the arrangement and strength of chemical bonds on the surface. Figure 2A, B, and C show the absorbance spectra of the surface at various stages of the surface modification procedure. Initially, treatment of glass with sulfuric acid resulted in surface activation, exposing silanol groups (Si–OH). The activated surface was then coated with 3-aminopropyltriethoxysilane (APTES) to yield an amine-functionalized siloxane group (–O–Si–O–), which is attributed to a peak at 1,045 cm^{-1} (Fig. 2A). Figure 2B shows the spectra of the glass surface after coating with poly(styrene-co-maleic anhydride) (PSMA) (red) compared with only PSMA in solution (blue). PSMA in solution (blue) shows two characteristic absorption peaks at 1,717 cm^{-1} and 1,749 cm^{-1} attributed to the ketone and anhydride group and a third one at 1,211 cm^{-1} characteristic of C-O-C bond of maleic anhydride (19, 20). However, in PSMA-coated glass surface (red), the peaks at 1,749 cm^{-1} and 1,211 cm^{-1} corresponding to maleic anhydride disappear, indicating covalent interaction between the anhydride groups with the amine group on APTES. We also observe a new peak at 760 cm^{-1} corresponding to styrene-ring puckering due to the zipper-like self-assembly of styrene groups of PSMA, which makes the surface hydrophobic.

Next, we treated this surface with poly-L-lysine (PLL) at a pH above its pI (8.3), such that the positively charged lysine groups ($-NH_3^+$) in PLL provided stable attachment of alginate gels on one end while bound to PSMA at the other. As shown in Fig. 2C, PLL in solution (blue) shows peaks at 3,333 cm^{-1} and 3,452 cm^{-1}, which correspond to primary and secondary amines, respectively. However, upon coating PLL on modified glass slides, these peaks disappeared (red), suggesting interaction of amine groups with the PSMA-coated surface by electrostatic and covalent binding (21). Since rapid gelation of alginate hydrogels requires a divalent cation, we used PLL mixed with barium chloride in the biofilm experiments. Thus, the PLL-$BaCl_2$ spots acted as "tie-layer" to bridge alginate matrix to the PSMA-coated surface (Fig. 2D). Finally, we confirmed that these surface modification processes resulted in a hydrophobic surface by contact angle goniometry,

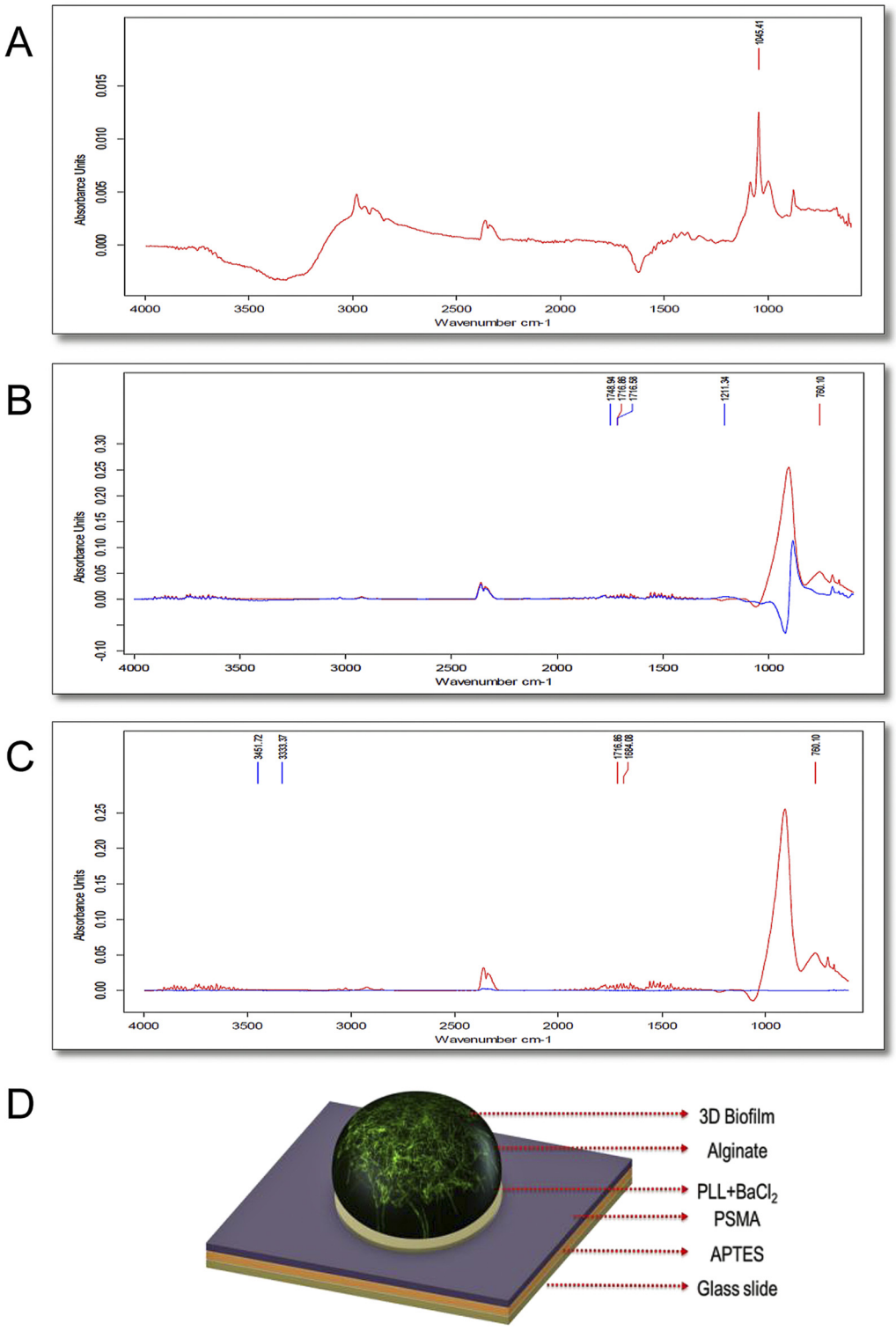

FIG 2 Fourier transform infrared (FTIR) spectroscopy analysis of surface modification. (A to C) Absorbance peaks of APTES (A), PSMA (B), and PLL (C) identified at different stages of surface modification, characterizing each layer of coating. (D) A schematic of a nano-biofilm spot on a modified glass slide.

wherein the alginate spots were nearly hemispherical, with a contact angle of 90.95° ± 2.75°.

Optimization of operating parameters. We optimized the various experimental conditions to obtain a robust and functional biofilm microarray using a two-level factorial design. Unlike single-factor experimental designs, wherein the outcomes of the process are assumed to depend on mutually independent single parameters, this statistical simulation study provides insights into

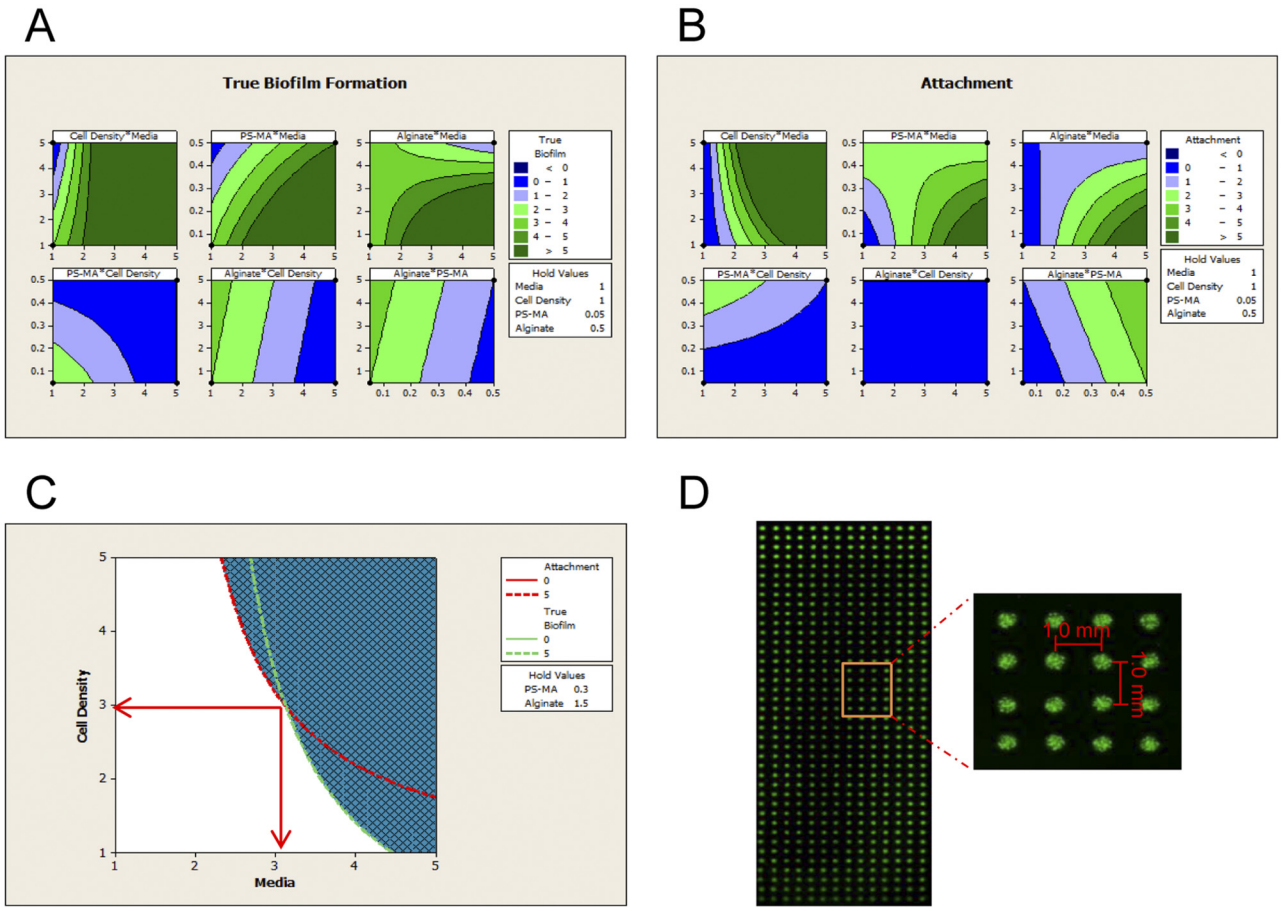

FIG 3 Factorial design of experiments for fabricating a robust microarray of nano-biofilms. (A and B) Interaction between the design variables—cell-seeding density, media, alginate, and PSMA—in forming true biofilms (A) and robust attachment of nano-biofilms (B). The y-x axes are labeled on top of each graph. (C) Optimal (blank) and nonoptimal (hatched) zones of robustly attached true biofilms at fixed concentrations of PSMA and alginate. Arrows represent favorable values for cell-seeding density and medium concentration. (D) Microarray scanner image of nano-biofilm microarray with 1,200 spots of identical nano-biofilms of 400-μm diameter.

the interaction between various experimental parameters (22). These experimental parameters or "design variables" determine the outcome or "response variables." As our goal is to obtain a robust biofilm microarray, we chose the response variables as measures of the robustness of the biofilm attachment to the glass surface and of the authenticity of the biofilm. These two response variables were assigned an arbitrary value of 0 (poor) to 5 (good) based on microscopic assessment. A robust attachment means that the biofilm did not detach even after 10 gentle washes. A "true" biofilm is defined by its idiosyncratic morphology, consisting of all three forms of fungi, namely, yeast cells, pseudohyphae, and hyphae, as evaluated by microscopy (23). In contrast, a "pseudobiofilm" consists of a random distribution of yeast and/or pseudohyphae. We chose the design variables as concentrations of media, alginate, PSMA coating, and cell-seeding density, since the preliminary experiments have shown that each of these experimental conditions had a profound impact on the response variables.

We evaluated the two response variables for the 16 (2^4) different experimental conditions corresponding to the two levels (low and high) of each of the four factors. We applied statistical analysis to these results using the Design of Experiments software (24) (Minitab Inc., State College, PA) to detect the interaction effects between the factors. The effects of the interactions between the four independent design variables on robust attachment and formation of true biofilms are shown in Fig. 3. Each panel of Fig. 3A represents the effect of interactions between any two design variables on true biofilm formation. For instance, from the first panel of Fig. 3A, we observe that cell-seeding density (*y* axis) and moderate to high medium concentration (*x* axis) favor biofilm formation. Similar analysis of other paired interactions (Fig. 3A) revealed that, while PSMA coating density had no effect, the concentrations of alginate matrix, media, and cell-seeding density played a pivotal role in the formation of biofilms. The biofilms were examined by light microscope to further delineate the conditions that favor true biofilms and not pseudobiofilms.

Similarly, we studied the effect of the paired interaction between design variables on robust attachment of the spots (Fig. 3B). We observed that the cell density and RPMI concentration did not contribute to the robust attachment of spots printed on the microarray, as it was governed only by the concentrations of alginate matrix and PSMA. With all the aforementioned independent interactions of factors, an overlay plot was generated and optimal parametric values were established for the concentrations of algi-

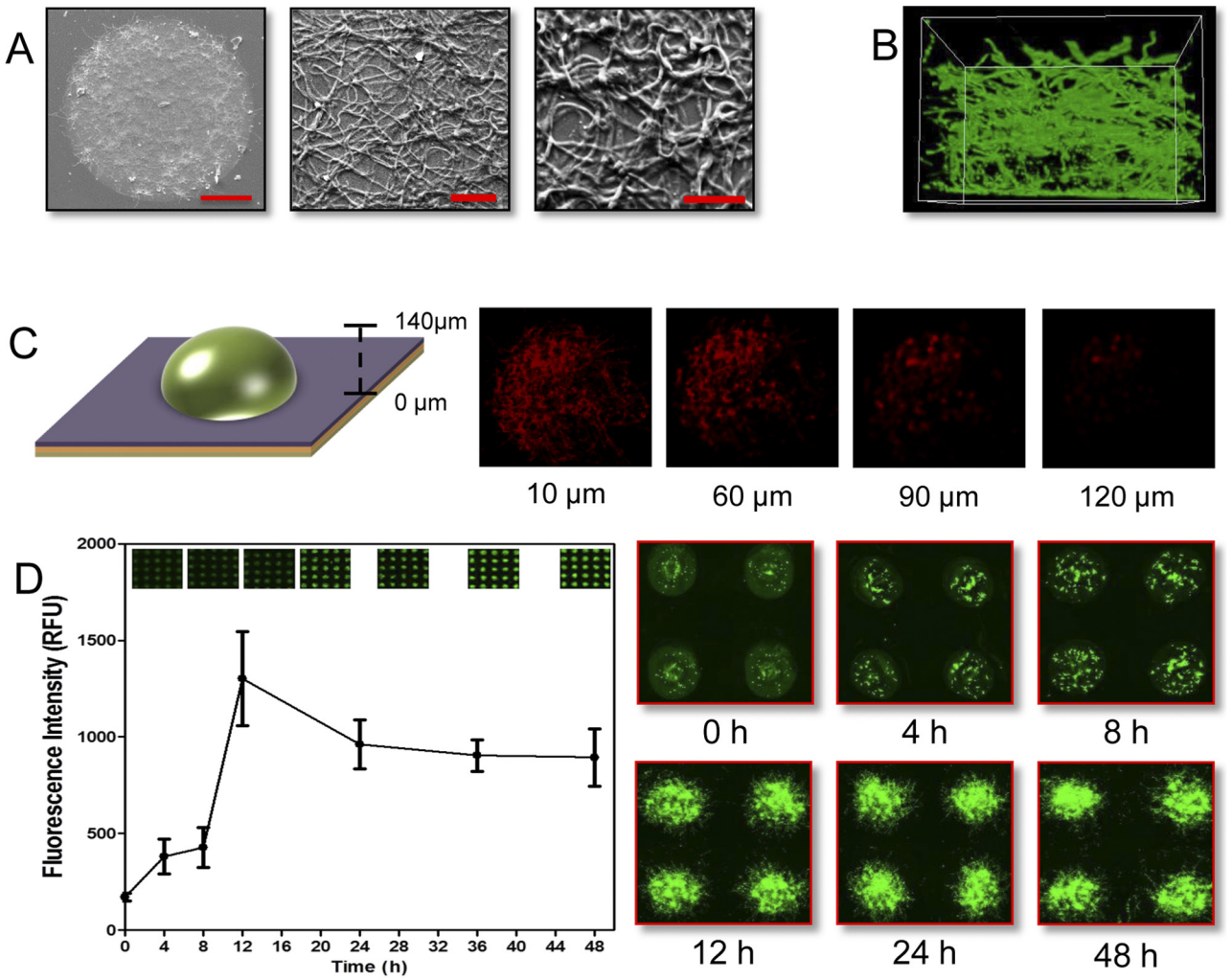

FIG 4 Characterization of nano-biofilms after 24 h of growth. (A) Scanning electron micrograph of a single spot of nano-biofilm at increasing magnifications (scale bars in the left, middle, and right panels are 100, 20, and 10 μm, respectively). Both filamentous and nonfilamentous morphologies can be identified. (B) Confocal laser scanning micrograph of a ConA staining demonstrates three-dimensional (3D) architecture. (C) Optical XY sections of different layers along the *z* axis, indicating a thickness of ~140 μm. (D) Growth kinetics over a period of 48 h along with microarray scanner images.

nate, media, cell-seeding density, and PSMA as 2%, 3×, 3 × 10^6 cells/ml, and 0.3%, respectively (Fig. 3C). Using these values, we robotically printed 1,200 spots (60 rows and 20 columns) of 30 nl each of *Candida albicans* yeast cells encapsulated in alginate matrix on modified glass microscope slides. The slide was incubated at 37°C for 24 h to allow for biofilm growth and maturation, yielding a nano-biofilm microarray (Fig. 3D). We observed that the spots remained hemispherical, attached robustly to the surface, and supported true biofilm growth.

Characterization of nano-biofilms. We characterized extensively the nano-biofilms grown on the microarray by scanning electron microscopy (SEM) and confocal laser scanning microscopy (CLSM) (Fig. 4). Using SEM, we observed that spherical yeast cells and filamentous hyphal elements were embedded in the alginate matrix (Fig. 4A). Using CLSM, we visualized the filamentous architecture of intact nano-biofilms by staining with fluorescent dye Concanavalin A (ConA), which selectively binds to mannose and glucose residues on cell wall polysaccharides (Fig. 4B). It can be seen from the cross-sectional view of the nano-biofilms (Fig. 4C) that the cells grew in three dimensions to a height of approximately 140 to 150 μm.

To quantify cell density in nano-biofilms, first, we measured the increase in fluorescence due to the uptake of FUN1 by metabolically active cells using a microarray scanner. We observed that the fluorescence from FUN1 correlated linearly with cell number over the range of interest (see Fig. S1A in the supplemental material). Additionally, we also confirmed that the levels of fluorescence at different spots on the microarray seeded with the same cell density were identical, indicating uniformity of biofilm growth at various spots on the microarray (Fig. S1B). Next, we established the kinetics of biofilm growth and maturation in alginate matrices using FUN1. As shown in Fig. 4D, the biofilm grew rapidly and maximum metabolic activity was reached within 12 h, after which the metabolic activity of the cell decreased, suggesting biofilm maturation. Therefore, the nano-biofilms grown in the microarray faithfully reproduced the standard 96-well plate model of biofilm formation (25), although with somewhat faster growth kinetics. The maturation of biofilm on the microarray

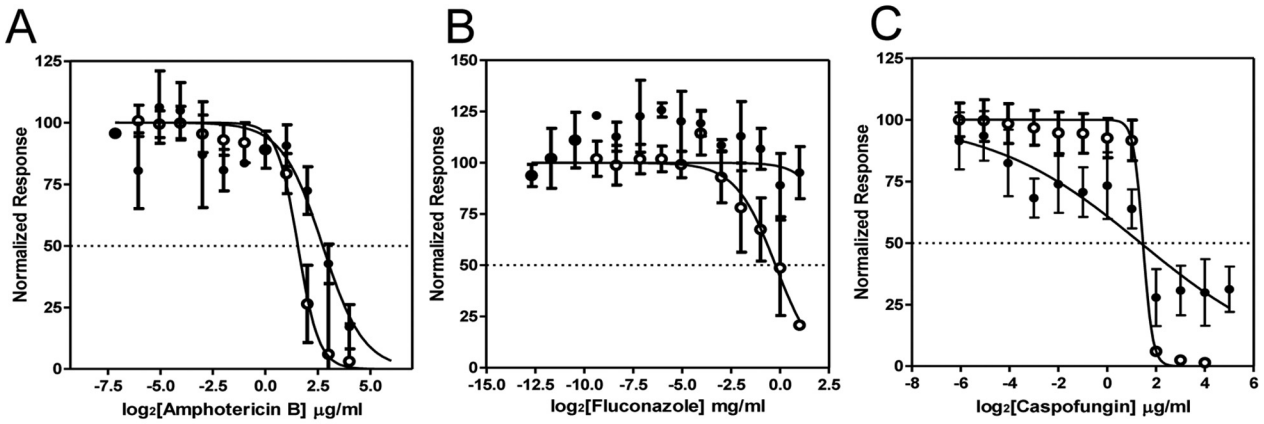

FIG 5 Profile of dose responses of nano-biofilms to common antifungal drugs. Data represent levels of susceptibility to amphotericin B (A), fluconazole (B), and caspofungin (C) in inhibiting biofilm formation (○) and against preformed biofilms (●). The normalized response refers to the percentage of metabolically active cells.

within 12 h was faster than the usual 24 h observed in 96-well plate, possibly because of the large (2,000-fold) reduction in the culture size (26, 27). It should also be noted that no additional medium was added to the microarray after initial seeding, in contrast to the well-plate models, wherein the biofilms are submerged in a large volume of media. These observations suggest that the nano-biofilm microarray offers the possibility of reducing the assay time and reagent volume in the assay protocol, thus increasing the throughput.

Susceptibility of nano-biofilms to antifungal drugs. Having ascertained that the morphological and growth characteristics of nano-biofilms on the microarray were comparable to those of the macroscopic biofilms grown in 96-well plates, we evaluated the response of nano-biofilms to clinically used antifungal drugs. In general, the formation and maturation of biofilm are associated with high levels of resistance to most known antifungal drugs (25, 28, 29). In particular, the susceptibility to azoles, a common class of antifungal drugs, exhibited by *C. albicans* in its planktonic morphology disappears after it matures into a biofilm. In fact, enhanced resistance of the biofilms to antifungal drugs is attributable as the most important reason for the high mortality rates associated with candidiasis (30, 31).

First, we confirmed that the response of the nano-biofilms to drugs was independent of their location on the microarray. We divided the microarray into seven identical blocks, and the nano-biofilms in each of the blocks were exposed for 24 h to quadruple increments in concentrations of amphotericin B, a commonly used antifungal agent. We observed that the nano-biofilms grown at different spatial locations on the microarray were identical in their response to the drug, further confirming consistency in the cell seeding, growth, and staining processes (see Fig. S2 in the supplemental material).

Next, we evaluated the antifungal susceptibility of biofilms and their planktonic counterparts that were encapsulated in alginate hydrogel matrix to three commonly used antifungal drugs belonging to different chemical classes. The effect of drug was determined from the fraction of the metabolically active cells that was remaining after 24 h of drug treatment compared to the controls and was reported as the drug concentration that inhibited the growth of biofilms to 50% (IC_{50}). As a proof of concept, we validated the susceptibility of nano-biofilms in the microarray against three commercially available antifungal agents belonging to three different chemical classes—amphotericin B (a polyene), fluconazole (an azole), and caspofungin (an echinocandin). To test the antifungal susceptibility of biofilms, the drugs were added 24 h after initial seeding of the microarray, during which period the biofilms grew and matured. To test the efficacy of drugs in preventing planktonic cells from forming biofilms, the drugs were added along with the cells during the initial seeding of the microarray. We observed that all three drugs were effective against planktonic cells in preventing biofilm formation (Fig. 5). However, when the drugs were tested against preformed biofilms, only amphotericin B and caspofungin, but not fluconazole, showed antifungal activity. The IC_{50}s of amphotericin B and caspofungin against preformed nano-biofilms were 1.0 μg/ml and 0.6 μg/ml, respectively, and these values are comparable to those obtained from macroscopic biofilms cultured in a 96-well plate (32, 33). The IC_{50} and IC_{80} values of the nano-biofilms for fluconazole were $>$1,024 μg/ml, which is also comparable to the results obtained from the 96-well plate model (32). Thus, the planktonic morphology of the fungi is susceptible to fluconazole but upon maturation to a biofilm displays a high degree of resistance. The intrinsic resistance to azoles is considered a hallmark of true biofilm formation and is attributed, among other reasons, to the binding of the azole compounds to β-glucans in the self-produced extracellular matrix of the biofilm (34). This phenomenon of azole resistance witnessed in the nano-biofilms but not in planktonic cells grown in the microarray provides additional phenotypic confirmation for biofilm formation. Thus, a 2,000-fold reduction in volume, in comparison with the 96-well plate model, had not impaired the formation of a true biofilm. These results attest that the nano-biofilm microarray is a veritable platform to study *C. albicans* biofilms. Of interest, we had reported earlier that the biofilms grown in a collagen matrix were resistant to caspofungin (18). This suggests that caspofungin, and probably other drugs with high affinity for proteins (35), may bind to collagen but not to an alginate matrix. Thus, despite its somewhat "artificial" nature, the chemically inert alginate matrix may be used as a universal scaffold for the encapsulation of biofilm cells and seems fully

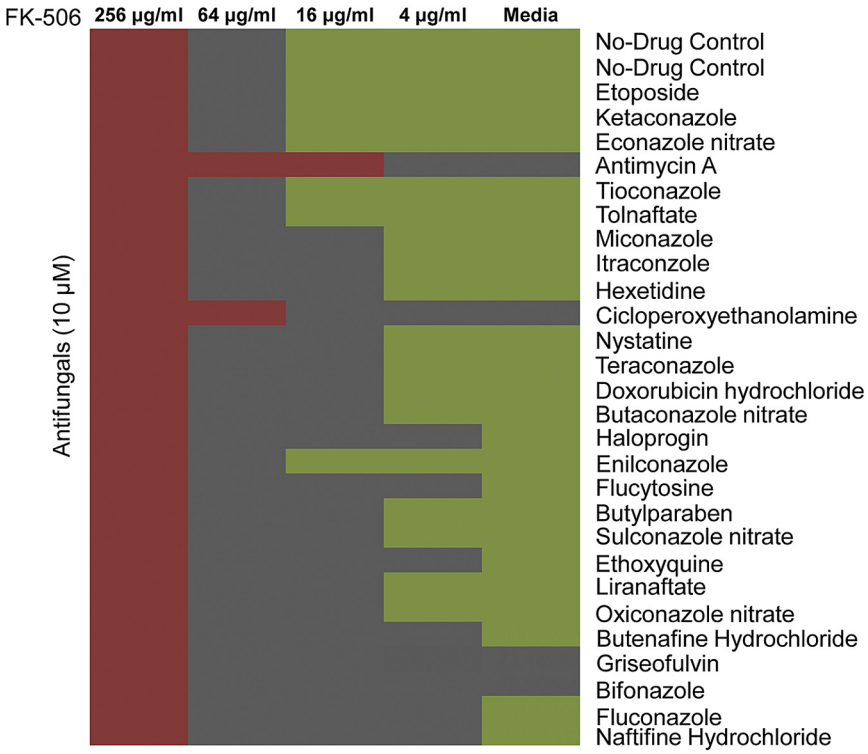

Independent hits	Combination hits
Antimycin A	Haloprogin
Cicloperoxyethanolamine	Flucytosine
Griseofulvin	Ethoxyquine
Bifonazole	Butenafine Hydrochloride
	Fluconazole
	Naftifine Hydrochloride

FIG 6 High-throughput combinatorial screening of antifungal drugs with FK506. A total of 28 antifungal drugs at 10 μM were tested in combination with 0 to 256 μg/ml FK506 in a checkerboard fashion, and the effect on biofilms was quantified. The drugs were classified based on the extent of biofilm inhibition: 0 to 25% (green); 25 to 50% (gray); and 50 to 100% (red). Four drugs were found to be effective singly, and six drugs were found to be effective in combination with 4 μg/ml of FK-506.

compatible with downstream applications during the drug discovery process.

Combinatorial screening of FDA-approved antifungal drug collection with FK506 for drug-drug interactions. A major difficulty in the treatment of *C. albicans* biofilm infections is that the biofilms are inherently resistant to most known antifungal agents compared to their planktonic counterparts. In particular, as shown in Fig. 5B, C. *albicans* biofilms are completely resistant to fluconazole. These biofilms are also resistant to other azoles, whereas the yeast cells are susceptible to this drug. Fluconazole targets an essential enzyme in the ergosterol biosynthetic pathway (36), and the biofilm resistance has been attributed to a reduction in the ergosterol levels in mature biofilms (34). It has been shown that calcineurin inhibitors such as FK506 or cyclosporin act synergistically with fluconazole and other azole drugs, making them fungicidal than fungistatic. FK506, or tacrolimus, is an immunosuppressant that is prescribed at low doses to patients undergoing organ transplants (37–39). Also, Uppuluri et al. have previously demonstrated the synergistic effect of calcineurin inhibitors and fluconazole against *C. albicans* biofilms (40). Thus, using FK506 in conjunction with existing antifungal drugs that are otherwise ineffective against biofilm infections offers an attractive possibility to treat invasive candidiasis.

We used the nano-biofilm microarray to examine the synergistic interaction between FK506 and antifungal drugs (Prestwick Chemicals, Washington, DC). This library consists of compounds that are FDA-approved, off-patent drugs (41). Hence, we tested the antifungal susceptibility of *C. albicans* biofilms against these drugs at 10 μM either individually or in combination with 0 to 256 μg/ml FK506 using amphotericin B as the positive control. Our miniaturized, high-throughput assay enabled us to evaluate the various combinations of the drugs, taken two at a time, as a checkerboard on a single microarray. In the absence of FK506, only four drugs, i.e., antimycin, cicloperoxyethanolamine, griseofulvin, and bifonazole, were effective against biofilms, confirming that the biofilms are resistant to most antifungal drugs which are reportedly potent in killing planktonic cells (Fig. 6). We observed that FK506 alone was active only at the highest concentration (256 μg/ml) (Fig. 6; see also Fig. S3 in the supplemental material) and that most of the drugs were effective when combined with higher concentrations ($\geq$16 μg/ml) of FK506 (Fig. 6). However, the addition of the lowest dose of FK506 (4 μg/ml or 5 nM) synergistically triggered antifungal activity with a number of drugs from various classes, including naftifine hydrochloride (allylamine), fluconazole, bificonazole (azoles), griseofulvin (benzofuran), ethoxyquin (quinolin), flucytosine (nucleoside analog), and haloprogin (phenyl ether). Taken together, the results from the combinatorial screening analysis have identified six new antifungal drugs that are ineffective against biofilm infections but can turn effective in synergistic combination with small doses of FK506. This provides a proof of concept of the nano-biofilm microarray for combinatorial drug screening.

Screening of NCI small-molecule library for novel antifungal drug candidates. To further validate the utility of the nano-biofilm microarray for HTS of novel antifungal drug candidates, we tested the presence of antifungal activity in the small molecules of the NCI 4256/36 challenge set. Since these compounds are reported to have anticancer activity, identification of antifungal activity in these compounds may be clinically desirable. We tested for antifungal activity of 57 compounds in this library against preformed biofilms at a single concentration of 5 μM. The screen

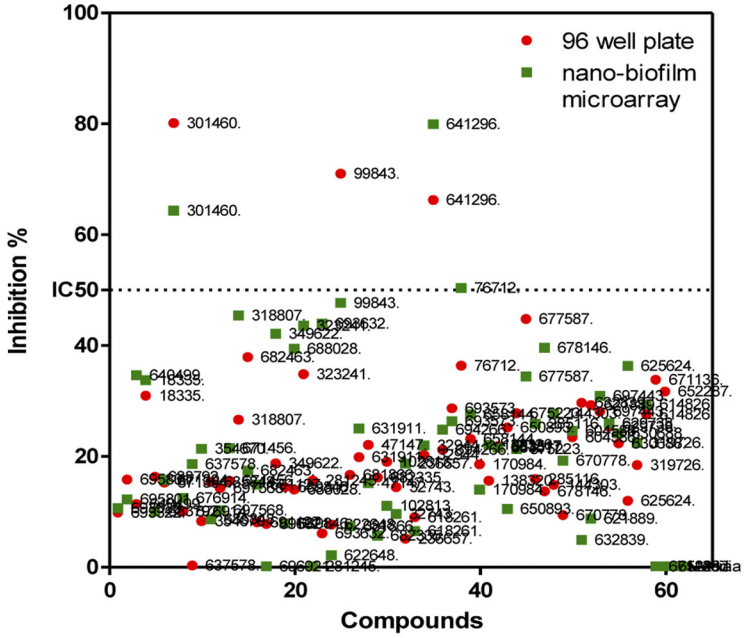

Compound	Inhibition (%)
Toyocamycin 99843	46.98 ± 0.95
Trichopolyn 301460	63.14 ± 1.69
Antineoplastic 641296	80.04 ± 2.91

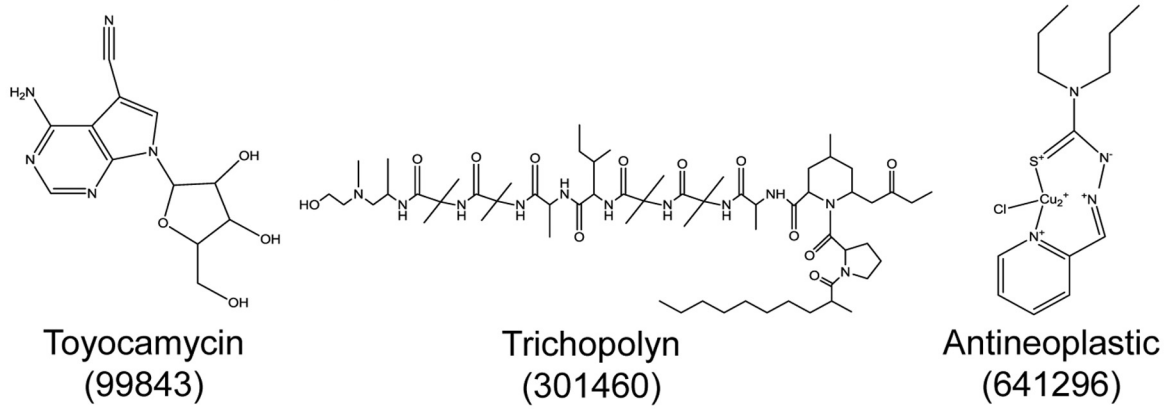

Toyocamycin (99843) Trichopolyn (301460) Antineoplastic (641296)

FIG 7 Screening of NCI challenge set 4256/36 for antibiofilm activity. Fifty-eight small-molecule compounds from the NCI challenge set were screened at 10 μM against preformed biofilms with the nano-biofilm microarray (green) or in a 96-well plate (red). Three hits were identified in the nano-biofilm microarray and were confirmed with the 96-well plate model.

included nano-biofilms treated without any drug-containing media as the negative control and a blank control without any cells to eliminate any background fluorescence. The high-throughput nature of the microarray enabled us to screen all compounds in 16 replicates totaling 1,200 assays on a single microarray slide. The screening results are shown in Fig. 7 along with the results from the industry standard 96-well plate for comparison. The compounds that inhibited the metabolic activity of biofilm by more than 50% compared to untreated controls were classified as "hits." Based on this criterion, we obtained three hits—01460, 99643, and 641296—from this library by both the microarray and the 96-well plate model. The three hits were toyocamycin (99843), trichopolyn (301460), and an antineoplastic (641296). Trichopolyn is a peptide antibiotic that has shown some promise as an immunosuppressant in *in vitro* experiments (42). It is derived from a fungus, *Trichoderma polysporum*, and the accepted mode of cell death is induction of membrane leakage. The antineoplastic (641296) is a less-studied hydrazinecarbothioamide compound. The hydrazinecarbiothioamide derivatives have shown antifungal and antitumor activity (43) and have been of interest as drug candidates as they have potential sites for binding to a variety of metal ions. Toyocamycin is an adenosine analog that has shown tumoricidal activity by inhibiting RNA synthesis and inducing apoptosis (44) and antibacterial activity by inhibiting kinase activity (45, 46). These three candidates may be investigated further for safety and efficacy in animal models of candidiasis.

It is appropriate to mention certain instances where conventional assays or further analyses may be warranted following a primary screen with the nano-biofilm microarray, such as studies focused on (i) specific inhibitors of native or organism-derived biofilm matrix, since the smallness of the nano-biofilms and encapsulation in an artificial alginate matrix in the microarray makes it difficult to isolate and quantify the effects of exopolymeric matrix components, including β-glucans and extracellular DNA; (ii) biofilm dispersion under flow conditions; and (iii) fungistatic drugs, which influence metabolic activity without affecting viability, since a metabolic stain may not accurately predict cell viability (47–51).

Conclusion. In summary, we have developed a high-throughput microarray for studying *C. albicans* biofilms. We demonstrated that despite more than 3 orders of magnitude of miniaturization, the morphological, phenotypic, and drug resistance characteristics of the nano-biofilms on the microarray are comparable to those of the macroscopic biofilms formed in 96-well plates. We also screened two small-molecule chemical libraries and identified novel antifungal drug candidates or novel combinations of existing drugs with antifungal activity. Although the microarray was developed for *Candida albicans* and was used for drug discovery, this universal platform is adaptable to other applications and offers numerous advantages, including the following. (i) Most currently used assays employ 96-well plates wherein the target biofilms are formed either in suspension or at the liquid-air interface and hence are easily disturbed during analysis procedures, resulting in false readouts. The microarray-based platform presented in this work employs robust porous hydrogel matrices, which not only support growth but also prevent the disruption and loss of biofilms during the experiments. (ii) Miniaturization of the assay from conventional microliter to nanoliter volumes reduces assay costs and time and enhances the feasibility of assays otherwise limited by valuable chemical or biological samples such as clinical isolates. (iii) Increases in throughput enable combinatorial screening of large number of samples. (iv) The platform offers ease of adaptability to mono- or polymicrobial bacterial and fungal cultures. (v) The platform is suitable for determining antimicrobial drug susceptibility in clinical settings.

MATERIALS AND METHODS

Culture conditions. *Candida albicans* strain SC5314, stored at −80°C in glycerol stock, was cultured on yeast extract-peptone-dextrose agar plates (YPD plates) and incubated at 37°C for 24 h. To obtain the growth of the budding yeast phenotype, a loopful of cells from fully grown YPD plates was subcultured in 20 ml of YPD liquid media and grown in an orbital shaker at 30°C for 12 to 18 h.

Fabrication of microarray slides. Borosilicate glass slides were rinsed in a staining jar with 99% ethanol and treated with concentrated sulfuric acid for 12 h. The slides were air-dried using a stream of nitrogen gas, rinsed with Milli-Q water, and baked at 80°C for 30 min. The slides were coated with 2.5% (wt/vol in toluene) 3-aminopropyltriethoxysilane (APTES) and baked at 120°C for 15 min, generating a layer of cross-linked APTES. Finally, the slides were spin coated with 0.3% (wt/vol in toluene) poly(styrene-comaleic anhydride) (PSMA) at 3,000 rpm for 30 s (52).

FTIR spectrometer analysis. Fourier transform infrared (FTIR) measurements were conducted on modified glass slides in the absorbance mode over a range of 4,000 to 400 cm^{-1} at a resolution of 4 cm^{-1} using a Tensor 27 instrument (Bruker Instruments). A high signal-to-noise ratio was achieved using 150 scans for each of the spectra, which were obtained at room temperature using a MIRacle Attenuated Total Reflection (ATR) accessory (Pike Instruments) with a diamond crystal. OPUS software was used to acquire and process the spectra.

Factorial design. To fabricate a robust nano-biofilm microarray that would support the growth of true biofilms, the experimental conditions were optimized by a two-level four-factor experimental design model (Minitab and Design of Experiment [DoE] software). The effect of experimental variables, including cell-seeding density, concentration media, PS-MA coating, and alginate matrix, was evaluated for two qualitative outcomes, namely, morphological characteristics of the biofilm (and its yield) and robust attachment of spots on slides. Thus, the cell-seeding density, media, and alginate matrix composition were established by the results of the DoE simulation.

Microarray printing. For preparation of inocula for printing and nano-biofilm formation in the microarray, cells harvested from overnight YPD cultures were washed twice and resuspended in sterile phosphate-buffered saline (PBS). The cell suspension was adjusted to a density of 5×10^6 cells/ml in RPMI 1640 and then added to alginate to give a final concentration of of 3×10^6 cells/ml in 1.5% alginate. The suspension containing yeast cells, alginate, and media was printed (30 nl per spot) on the functionalized PSMA-coated glass slides using a noncontact microarray spotter (Omnigrid Micro, Digilab Inc., Holliston, MA) with conically tapered 100-μm-long orifice ceramic tips. An array of 60 rows and 20 columns was printed at room temperature with relative humidity of 100%. In a standard print run, the tips were primed, rinsed in running water, and vacuum dried twice after each sample-loading and printing step. The slides were then placed in a humidified hybridization cassette (Arrayit, Sunnyvale, CA) to prevent evaporation of spots and incubated at 37°C. All microarrayer functions such as sample loading, priming, printing, and spatial distribution of the array were controlled by AxSys programming (Digilab).

Microscopy. The morphology, distribution, and topography of the nano-biofilms grown were routinely monitored by inverted-light microscopy. The architecture of the alginate matrix scaffolding the yeast cells and the biofilm was imaged using a Zeiss EVO 40 scanning electron microscope (Carl Zeiss, Thornwood, NY). Briefly, the biofilms formed in the microarray were fixed with a solution of glutaraldehyde (2.5% [wt/vol])-0.1 M sodium cacodylate buffer at pH 7.4 for 2 h at 37°C. Following fixation, the biofilms were treated with a solution of osmium tetroxide (1% [wt/vol])-0.1 M sodium cacodylate buffer at pH 7.4 for 2 h at room temperature. The samples were rinsed with water and soaked in a graded series of ethanol solutions (a step gradient of 30%, 50%, 70%, and 90% in water for 10 min per step), ending with 100% ethanol. After dehydration, the samples were dried overnight in a vacuum dryer and subsequently coated with a 60:40 gold-palladium alloy, approximately 10 nm thick, using a Cressington sputter coater for a duration of 30 s.

For determining the three-dimensional morphology of the nano-biofilms grown on the microarray, Concanavalin A, a fluorescent stain (Invitrogen Corp., Carlsbad, CA), was used and imaged using an LSM 510 confocal scanning laser microscope (CSLM) (18) (Carl Zeiss).

Viability assay. The viability of nano-biofilms was determined based on their metabolic activity, using FUN 1 fluorescent dye. Upon staining, the fluorescent dye is internalized and processed only by metabolically active fungal cells. The excitation and emission spectra of FUN 1, 480 to 535/550 nm, are compatible with the sets of lasers [523 nm with a Photo Multiplier Tube gain (PMT) of 300] and filters installed in most microarray scanners. The nano-biofilms were stained with 0.5 mM FUN 1, by simply immersing the entire microarray slide in a staining jar, and incubated in the dark at 37°C for 30 min. Following incubation, the microarray slide was washed three times by immersion in phosphate-buffered saline (PBS) to remove excess stain, air-dried, and scanned in a microarray scanner (GenePix Personal 4100A; Axon Instruments, Union City, CA). Images were analyzed with GenePix Pro V7 (Axon Instruments, Union City, CA).

Susceptibility testing using nano-biofilm microarray. The stock solutions of the antifungal drugs amphotericin B and caspofungin were diluted in RPMI 1640-PBS to a maximum concentration of 16 μg/ml and fluconazole to a maximum concentration of 2 mg/ml. The subsequent dilutions were made from the stock solutions in RPMI 1640. Using the robotic arrayer, 30 nl of drugs, in 4-fold dilutions of starting concentrations, were printed on top of the nano-biofilms to study the effect of drugs on biofilm inhibition. In another experiment, to study the effect of drugs in preventing biofilm formation, 30 nl of drugs at similar concentrations were printed on top of the cells before they formed biofilms. The microarray(s) containing drugs was then incubated in a humidified hybridization cassette for 24 h, gently washed in PBS, stained with FUN 1, and analyzed using the microarray scanner.

To prepare the dose-response curve, the relative fluorescence unit (RFU) values were converted into normalized response values. Briefly, the values of fluorescence intensity of the control and dead (killed with

10 μg/ml amphotericin B) biofilms were arbitrarily set at 100% and 0%, respectively, and the inhibitory effects of compounds were determined by the reduction in fluorescence intensity in relation to the controls. The IC_{50} (the inhibitory concentration of drugs required to reduce the fluorescence intensity by half compared to the live control level) values were determined by fitting the normalized values to the variable slope Hill equation (an equation determining the nonlinear drug dose-response relationship) using GraphPad Prism software (La Jolla, CA).

Combinatorial screening of a collection of FDA-approved antifungal drugs with FK506. A stock solution of FK506 (Sigma) was prepared at 10 mg/ml in dimethyl sulfoxide (DMSO) and stored at −80°C until use. FK506 was diluted to a final concentration of 8 mg/ml just prior to use, and 30 nl was spotted on top of the preformed biofilms on the microarray. A total of 28 antifungal drugs from Prestwick Chemicals Ltd. (Washington, DC) stored at −80°C in DMSO were diluted to a final concentration of 10 μM just prior to use, and 30 nl of each reaction volume was spotted on top of the preformed biofilms on the microarray. The microarray was incubated for 24 h, stained with FUN1, and analyzed for viability as described above.

Screening of small-molecule NCI challenge set 4256/36 chemical library. NCI challenge set 4256/36, a drug library of 57 small molecules with suitable positive (media) and negative (DMSO) controls, acquired from National Cancer Institute, was stored at −80°C until use. Just prior to printing, the drugs were diluted to 20 μM in RPMI 1640. Drugs (30 nl) were printed on top of preformed biofilms and were incubated in humidification cassettes for 24 h at 37°C, washed, stained, and scanned as described above. The drugs that resulted in <50% cell viability compared to the control without drugs were identified as representing a "hit."

To screen for antifungal activity using a 96-well plate, the inoculum was adjusted to a density of 1×10^6 cells/ml in RPMI 1640. A 100-μl volume of cell suspension was added to each well of a tissue culture-treated, flat-bottom 96-well plate and incubated at 37°C. After 24 h, the biofilms were washed with PBS to remove any nonadherent cells. To the biofilms formed, 100 μl of drugs at 10 μM from the NCI challenge set was added and incubated at 37°C for additional 24 h. After drug treatment, the viability of the biofilms was measured using an XTT assay (32).

SUPPLEMENTAL MATERIAL

Supplemental material for this article may be found at http://mbio.asm.org/lookup/suppl/doi:10.1128/mBio.00331-13/-/DCSupplemental.

Figure S1, TIF file, 0.1 MB.
Figure S2, TIF file, 0.2 MB.
Figure S3, TIF file, 0.1 MB.

ACKNOWLEDGMENTS

This work was funded in part by the U.S. Army Medical Research and Materiel Command, Combat Casualty Care Research Directorate intramural funding program, from the Institute for Integration of Medicine and Science (UL 1RR025767) of the National Center for Research Resources. Biofilm-related work in the J.L.L.-R. laboratory is funded by NIH (1R01DE023510-01) and by the Department of Defense (W911NF-11-1-0136), and infectious disease-related work in the A.K.R. laboratory is funded by NIH (SC1HL112629). Confocal microscopy was performed at the Research Center for Minority Institutions (RCMI.) Advance Imaging Center, supported by grant 5G12 RR01 3646-10.

K.P.L. is an employee of the U.S. government. The work presented is part of his official duty.

The opinions or assertions contained herein are our private views and are not to be construed as official or as reflecting the views of the Department of the Army or the Department of Defense or the NIH.

A.S. designed and performed the experiments, analyzed data, and wrote the paper. K.P.L. contributed to reagents and data analysis. J.L.L.-R. and A.K.R. conceived the study and contributed to data analysis and manuscript preparation. We all read and approved the final manuscript.

REFERENCES

1. **Edmond MB, Wallace SE, McClish DK, Pfaller MA, Jones RN, Wenzel RP.** 1999. Nosocomial bloodstream infections in United States hospitals: a three-year analysis. Clin. Infect. Dis. **29:**239–244.
2. **Pittet D, Li N, Woolson RF, Wenzel RP.** 1997. Microbiological factors influencing the outcome of nosocomial bloodstream infections: a 6-year validated, population-based model. Clin. Infect. Dis. **24:**1068–1078.
3. **Wenzel RP, Edmond MB.** 2001. The impact of hospital-acquired bloodstream infections. Emerg. Infect. Dis. **7:**174–177.
4. **Wisplinghoff H, Bischoff T, Tallent SM, Seifert H, Wenzel RP, Edmond MB.** 2004. Nosocomial bloodstream infections in US hospitals: analysis of 24,179 cases from a prospective nationwide surveillance study. Clin. Infect. Dis. **39:**309–317.
5. **Wenzel RP.** 2004. The antibiotic pipeline—challenges, costs, and values. N. Engl. J. Med. **351:**523–526.
6. **Gan M, Tang Y, Shu Y, Wu H, Chen L.** 2012. Massively parallel bacterial and yeast suspension culture on a chip. Small **8:**863–867.
7. **Luo X, Shen K, Luo C, Ji H, Ouyang Q, Chen Y.** An automatic microturbidostat for bacterial culture at constant density. Biomed Microdevices 2010:499–503.
8. **Weibel DB, DiLuzio WR, Whitesides GM.** 2007. Microfabrication meets microbiology. Nat. Rev. Microbiol. **5:**209–218.
9. **Balagaddé FK, You L, Hansen CL, Arnold FH, Quake SR.** 2005. Long-term monitoring of bacteria undergoing programmed population control in a microchemostat. Science **309:**137–140.
10. **Hong SH, Hedge M, Kim J, Wang X, Jayaraman A, Wood TK.** 2012, Synthetic quorum-sensing circuit to control consortial biofilm formation and dispersal in a microfluidic device. Nat. Commun. **3:**613.
11. **Keymer JE, Galajda P, Muldoon C, Park S, Austin RH.** 2006. Bacterial metapopulations in nanofabricated landscapes. Proc. Natl. Acad. Sci. U. S. A. **103:**17290–17295.
12. **Mao H, Cremer PS, Manson MD.** 2003. A sensitive, versatile microfluidic assay for bacterial chemotaxis. Proc. Natl. Acad. Sci. U. S. A. **100:**5449–5454.
13. **Borisy AA, Elliott PJ, Hurst NW, Lee MS, Lehar J, Price ER, Serbedzija G, Zimmermann GR, Foley MA, Stockwell BR, Keith CT.** 2003. Systematic discovery of multicomponent therapeutics. Proc. Natl. Acad. Sci. U. S. A. **100:**7977–7982.
14. **Balaban NQ, Merrin J, Chait R, Kowalik L, Leibler S.** 2004. Bacterial persistence as a phenotypic switch. Science **305:**1622–1625.
15. **Zhang L, Yan K, Zhang Y, Huang R, Bian J, Zheng C, Sun H, Chen Z, Sun N, An R, Min F, Zhao W, Zhuo Y, You J, Song Y, Yu Z, Liu Z, Yang K, Gao H, Dai H, Zhang X, Wang J, Fu C, Pei G, Liu J, Zhang S, Goodfellow M, Jiang Y, Kuai J, Zhou G, Chen X.** 2007. High-throughput synergy screening identifies microbial metabolites as combination agents for the treatment of fungal infections. Proc. Natl. Acad. Sci. U. S. A. **104:**4606–4611.
16. **LaFleur MD, Lucumi E, Napper AD, Diamond SL, Lewis K.** 2011. Novel high-throughput screen against *Candida albicans* identifies antifungal potentiators and agents effective against biofilms. J. Antimicrob. Chemother. **66:**820–826.
17. **Eun YJ, Weibel DB.** 2009. Fabrication of microbial biofilm arrays by geometric control of cell adhesion. Langmuir **25:**4643–4654.
18. **Srinivasan A, Uppuluri P, Lopez-Ribot J, Ramasubramanian AK.** 2011. Development of a high-throughput *Candida albicans* biofilm Chip. PLoS ONE **6:**e19036. doi: 10.1371/journal.pone.0019036.
19. **Al-Sabagh AM, Noor El-Din MR, Morsi RE, Elsabee MZ.** 2009. Styrene-maleic anhydride copolymer esters as flow improvers of waxy crude oil. J. Petrol. Sci. Eng. **65:**139–146.
20. **Kyeremateng SO, Amado E, Kressler J.** 2007. Synthesis and characterization of random copolymers of (2,2-dimethyl-1,3-dioxolan-4-yl)methyl methacrylate and 2,3-dihydroxypropyl methacrylate. Eur. Polym. J. **43:**3380–3391.
21. **Ivanova EP, Pham DK, Brack N, Pigram P, Nicolau DV.** 2004. Poly(L-lysine)-mediated immobilisation of oligonucleotides on carboxy-rich polymer surfaces. Biosens. Bioelectron. **19:**1363–1370.
22. **Chen Y, Bloemen V, Impens S, Moesen M, Luyten FP, Schrooten J.** 2011. Characterization and optimization of cell seeding in scaffolds by factorial design: quality by design approach for skeletal tissue engineering. Tissue Eng. Part C Methods **17:**1211–1221.
23. **Chandra J, Kuhn DM, Mukherjee PK, Hoyer LL, McCormick T, Ghannoum MA.** 2001. Biofilm formation by the fungal pathogen *Candida*

albicans: development, architecture, and drug resistance. J. Bacteriol. **183:** 5385–5394.
24. **Dong J, Mandenius CF, Lübberstedt M, Urbaniak T, Nüssler AK, Knobeloch D, Gerlach JC, Zeilinger K.** 2008. Evaluation and optimization of hepatocyte culture media factors by design of experiments (DoE) methodology. Cytotechnology **57:**251–261.
25. **Sanglard D, Odds FC.** 2002. Resistance of Candida species to antifungal agents: molecular mechanisms and clinical consequences. Lancet Infect. Dis. **2:**73–85.
26. **Yeater KM, Chandra J, Cheng G, Mukherjee PK, Zhao X, Rodriguez-Zas SL, Kwast KE, Ghannoum MA, Hoyer LL.** 2007. Temporal analysis of Candida albicans gene expression during biofilm development. Microbiology **153:**2373–2385.
27. **Blankenship JR, Mitchell AP.** 2006. How to build a biofilm: a fungal perspective. Curr. Opin. Microbiol. **9:**588–594.
28. **Jabra-Rizk MA, Falkler WA, Meiller TF.** 2004. Fungal biofilms and drug resistance. Emerg. Infect. Dis. **10:**14–19.
29. **Kuhn DM, Ghannoum MA.** 2004. *Candida* biofilms: antifungal resistance and emerging therapeutic options. Curr. Opin. Investig. Drugs **5:**186–197.
30. **Ramage G, Mowat E, Jones B, Williams C, Lopez-Ribot J.** 2009. Our current understanding of fungal biofilms. Crit. Rev. Microbiol. **35:** 340–355.
31. **Ramage G, Martínez JP, López-Ribot JL.** 2006. *Candida* biofilms on implanted biomaterials: a clinically significant problem. FEMS Yeast Res. **6:**979–986.
32. **Ramage G, Vande Walle K, Wickes BL, López-Ribot JL.** 2001. Standardized method for in vitro antifungal susceptibility testing of Candida albicans biofilms. Antimicrob. Agents Chemother. **45:**2475–2479.
33. **Bachmann SP, VandeWalle K, Ramage G, Patterson TF, Wickes BL, Graybill JR, López-Ribot JL.** 2002. In vitro activity of caspofungin against *Candida albicans* biofilms. Antimicrob. Agents Chemother. **46:** 3591–3596.
34. **Mukherjee PK, Chandra J, Kuhn DM, Ghannoum MA.** 2003. Mechanism of fluconazole resistance in Candida albicans biofilms: phase-specific role of efflux pumps and membrane sterols. Infect. Immun. **71:** 4333–4340.
35. **Paderu P, Garcia-Effron G, Balashov S, Delmas G, Park S, Perlin DS.** 2007. Serum differentially alters the antifungal properties of echinocandin drugs. Antimicrob. Agents Chemother. **51:**2253–2256.
36. **Steinbach WJ, Reedy JL, Cramer RA, Perfect JR, Heitman J.** 2007. Harnessing calcineurin as a novel anti-infective agent against invasive fungal infections. Nat. Rev. Microbiol. **5:**418–430.
37. **Robbins N, Uppuluri P, Nett J, Rajendran R, Ramage G, Lopez-Ribot JL, Andes D, Cowen LE.** 2011. Hsp90 governs dispersion and drug resistance of fungal biofilms. PLoS Pathog. **7:**e1002257. doi: 10.1371/journal.ppat.1002257.
38. **Marchetti O, Entenza JM, Sanglard D, Bille J, Glauser MP, Moreillon P.** 2000. Fluconazole plus cyclosporine: a fungicidal combination effective against experimental endocarditis due to *Candida albicans*. Antimicrob. Agents Chemother. **44:**2932–2938.
39. **Reedy JL, Husain S, Ison M, Pruett TL, Singh N, Heitman J.** 2006. Immunotherapy with tacrolimus (FK506) does not select for resistance to calcineurin inhibitors in Candida albicans isolates from liver transplant patients. Antimicrob. Agents Chemother. **50:**1573–1577.
40. **Uppuluri P, Nett J, Heitman J, Andes D.** 2008. Synergistic effect of calcineurin inhibitors and fluconazole against *Candida albicans* biofilms. Antimicrob. Agents Chemother. **52:**1127–1132.
41. **Okoli I, Coleman JJ, Tampakakis E, Tempakakis E, An WF, Holson E, Wagner F, Conery AL, Larkins-Ford J, Wu G, Stern A, Ausubel FM, Mylonakis E.** 2009. Identification of antifungal compounds active against *Candida albicans* using an improved high-throughput *Caenorhabditis elegans* assay. PLoS One **4:**e7025. doi: 10.1371/journal.pone.0007025.
42. **De Lucca AJ, Walsh TJ.** 1999. Antifungal peptides: novel therapeutic compounds against emerging pathogens. Antimicrob. Agents Chemother. **43:**1–11.
43. **Opletalová V, Kalinowski DS, Vejsová M, Kunes J, Pour M, Jampílek J, Buchta V, Richardson DR.** 2008. Identification and characterization of thiosemicarbazones with antifungal and antitumor effects: cellular iron chelation mediating cytotoxic activity. Chem. Res. Toxicol. **21:** 1878–1889.
44. **Park HY, Kim MK, Moon SI, Cho YH, Lee CH.** 2006. Cell cycle arrest and apoptotic induction in LNCaP cells by MCS-C2, novel cyclin-dependent kinase inhibitor, through p53/p21WAF1/CIP1 pathway. Cancer Sci. **97:**430–436.
45. **Long MC, Parker WB.** 2006. Structure-activity relationship for nucleoside analogs as inhibitors or substrates of adenosine kinase from *Mycobacterium tuberculosis*. I. Modifications to the adenine moiety. Biochem. Pharmacol. **71:**1671–1682.
46. **Kiburu IN, LaRonde-LeBlanc N.** 2012. Interaction of Rio1 kinase with toyocamycin reveals a conformational switch that controls oligomeric state and catalytic activity. PLoS One **7:**e37371. doi: 10.1371/journal.pone.0037371.
47. **Teal TK, Lies DP, Wold BJ, Newman DK.** 2006. Spatiometabolic stratification of *Shewanella oneidensis* biofilms. Appl. Environ. Microbiol. **72:** 7324–7330.
48. **Renye JA, Piggot PJ, Daneo-Moore L, Buttaro BA.** 2004. Persistence of *Streptococcus mutans* in stationary-phase batch cultures and biofilms. Appl. Environ. Microbiol. **70:**6181–6187.
49. **Uppuluri P, Srinivasan A, Ramasubramanian A, Lopez-Ribot JL.** 2011. Effects of fluconazole, amphotericin B, and caspofungin on *Candida albicans* biofilms under conditions of flow and on biofilm dispersion. Antimicrob. Agents Chemother. **55:**3591–3593.
50. **Martins M, Henriques M, Lopez-Ribot JL, Oliveira R.** 2012. Addition of DNase improves the in vitro activity of antifungal drugs against *Candida albicans* biofilms. Mycoses **55:**80–85.
51. **Martins M, Uppuluri P, Thomas DP, Cleary IA, Henriques M, Lopez-Ribot JL, Oliveira R.** 2010. Presence of extracellular DNA in the *Candida albicans* biofilm matrix and its contribution to biofilms. Mycopathologia **169:**323–331.
52. **Srinivasan A, Lopez-Ribot JL, Ramasubramanian AK.** 2012. Candida albicans biofilm Chip (CaBChip) for high-throughput antifungal drug screening. J. Vis. Exp. **65:**e3845.